Volume 1 | Number 1 | Jan 2013 | Pages 1–100

ROYAL SOCIETY OF CHEMISTRY

This is an *Accepted Manuscript*, which has been through the Royal Society of Chemistry peer review process and has been accepted for publication.

Accepted Manuscripts are published online shortly after acceptance, before technical editing, formatting and proof reading. Using this free service, authors can make their results available to the community, in citable form, before we publish the edited article. We will replace this *Accepted Manuscript* with the edited and formatted *Advance Article* as soon as it is available.

You can find more information about *Accepted Manuscripts* in the **Information for Authors**.

Please note that technical editing may introduce minor changes to the text and/or graphics, which may alter content. The journal's standard **Terms & Conditions** and the **Ethical guidelines** still apply. In no event shall the Royal Society of Chemistry be held responsible for any errors or omissions in this *Accepted Manuscript* or any consequences arising from the use of any information it contains.

Journal Name

COMMUNICATION

A linear fluorescence-quenching response in an amidine-functionalised solid-state sensor for gas-phase and aqueous CO$_2$ detection

A. Das[a] and D. M. D'Alessandro*[a]

An amidine-functionalised metal-organic framework (MOF) was shown to be an effective chemosensor in the presence of gaseous and aqueous phase CO$_2$ by virtue of a quenched fluorescence response. This work demonstrates how multifunctional MOFs with high selectivity for CO$_2$ may be exploited to develop CO$_2$ chemosensors.

Introduction

Changes in the natural world arising from increasing carbon dioxide emissions due to the industrial revolution necessitate the development of CO$_2$ sensors in both the gas phase (e.g., to monitor CO$_2$ concentrations in the air) and in solution state (e.g., to monitor CO$_2$ concentrations in the ocean). In particular, the presence of carbon dioxide in confined space environments (e.g., mines, wells, regions of volcanic eruptions, sewers, submarines) has been a continual human health problem. Currently, detection and quantification of CO$_2$ gas are performed using spectroscopic techniques (e.g., IR and GC-MS) or electrochemical methods, while NDIR-based sensors have been developed to monitor CO$_2$ concentrations in the ocean in order to monitor the effects of increased atmospheric CO$_2$ on the global carbon cycle. These techniques are problematic in that they are power-intensive and can be bulky and expensive.[1, 2]

Metal-organic frameworks (MOFs) have garnered much attention for their potential applications in CO$_2$ capture,[3, 4] and an important strategy in the development of such MOFs has involved the inclusion of specific functional sites to improve the uptake, selectivity and heat of adsorption. MOFs are also capable of possessing numerous synergistic functions; for example, the presence of fluorophoric functional sites or guest

molecules could allow for the visual detection of the presence or absence of CO$_2$ molecules in a framework. Fluorophoric "reporter" sites can be classed into two groups, in which (i) CO$_2$ changes the structural conformation of the fluorophoric reporter molecule and hence its fluorescence properties, e.g., distyrylbenzene,[5] dipropylamine/hexaphenylsilole solution,[6] 5-amino-1-pentanol/DBU/tetraphenylethene solution[7] (the
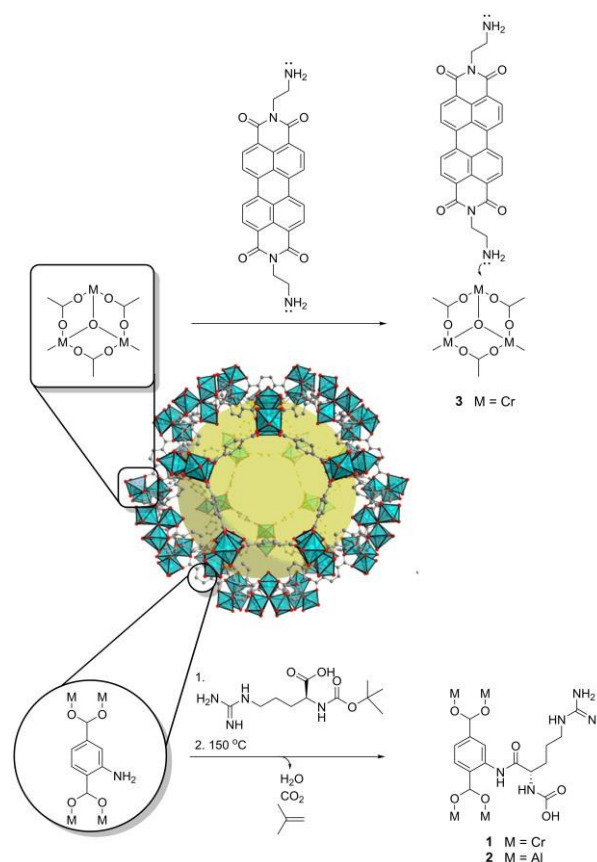

Figure 1. Schematic diagram showing PSM reactions carried out to affect perylene (top) and amidine (bottom) functionalisation. Figure adapted from reference 10.

[a.] *School of Chemistry F11, University of Sydney, Australia 2006.*
†Electronic Supplementary Information (ESI) available: [details of any supplementary information available should be included here]. See DOI: 10.1039/x0xx00000x

Table 1 Summary of gas adsorption data for compounds 1, 2 and 3.

Compound	BET surface area (m^2/g)	Pore volume (cm^3/g)	$|Q_{st}|$ (kJ/mol)	CO$_2$ uptake[†]		S
				mmol/g	mmol/cm^3	
1	798.1±21.59	0.36	28.8	0.94	1.01	11.6
2	770.1±14.61	0.31	34.7	1.22	1.25	16.7
3	677.8±18.73	0.29	26.7	0.55	0.79	14.3

latter two are due to aggregation-induced emission processes of the fluorophore from the reaction of CO_2 with the amine/amidine); or (ii) CO_2 chemically reacts with the moiety, changing its electronic and fluorescence properties, e.g., substituted perylenes,[8] guanidines and amidines.[9]

While the first strategy has been reported in MOFs,[5] the second has thus far only been documented in solution state, ionic liquids and in polymers.[11, 12] Through the incorporation of a site that reacts or interacts with CO_2 (and in doing so, changes its fluorescence properties) into a porous framework with high CO_2 selectivity, one could envision a highly sensitive CO_2 detector.

Amidines and amines have been investigated extensively for their CO_2 sensing abilities due to their reactivity with CO_2.[7, 9, 13, 14] They have been exploited for this purpose by covalently binding the moiety to fluorophores or chromophores such as perylenes and spiropyrans.[8, 15] Investigations into the reactivity of amidines with CO_2 in the context of MOFs have not been reported in the literature to the best of our knowledge. Perylene bisimides covalently bonded with amine or amidine functionalities have been shown to change both their UV-visible and fluorescence emission properties in response to small quantities of dissolved CO_2 in the solution state.[8] This process occurs through the reaction of acidic CO_2 with the basic nitrogen lone pair, resulting in a charged species which alters the electronic properties of the perylene unit (and therefore, its UV-visible and fluorescence properties).

Herein, we exploit the potential multifunctional and synergistic functions in MOFs to synthesise a solid state CO_2 chemosensor (*i.e.*, a material that transduces a specific chemical stimulus in the environment to a detectable signal). A particular emphasis is the interplay between porosity, CO_2 reactivity with functional sites in the MOF and the resulting impact on the fluorescence properties. The MOF employed in the present work, MIL-101-NH$_2$, has been extensively investigated for its ability to be functionalised and its adsorption properties.[16] The amidine and perylene functionalities previously employed in solution state,[15, 17] ionic liquid[7] and polymeric[8, 13, 14] CO_2 sensors have been further exploited here.

The incorporation of reactive amine (or amidine) moieties into a MOF scaffold can be problematic due to the unforeseeable ways in which the functional group may disrupt the self-assembly process. In addition, the synthetically challenging nature of incorporating such functionalities covalently into the ligand backbone itself (in the presence of other metal binding/ligating groups), can often prove unsurmountable. A post-synthetic modification (PSM) approach was hence adopted here to incorporate the 2,2'-(1,3,8,10-tetrahydroanthra[2,1,9-def:6,5,10-d'e'f']diisoquinoline-2,9-diyl)bis(ethan-1-amine) (peda) and arginine moieties into the robust and porous M-MIL-101 (where M = Cr, Al) scaffold.[18, 19]

The amidine functional group was incorporated using a condensation PSM reaction between the carboxylic acid terminus of the amino acid arginine and the NH$_2$ functionality of the MOF. This procedure was carried out using a coupling reagent well-known in peptide chemistry, diisocarbodiimide (DIC),[20] which has recently been applied to MOFs.[21] This reaction requires BOC protection of the terminal NH$_2$ group of the amino acid, which can be easily removed following PSM *via* thermolysis (Figure S1).[22] The peda moiety was incorporated using an open metal site ligation PSM approach, which has previously been applied to primary[23, 24] and secondary amines.[25-28] This strategy is perhaps the simplest synthetic approach to incorporating symmetrical amines or amine-containing moieties, as one end of the molecule binds to the open metal site leaving the other free in the pore to interact with incoming guest molecules (Figure S2). This approach has recently been employed to incorporate a pyridyl-functionalised perylene moiety into Cr-MIL-101.[29]

Results and discussion

BOC-Arg-OH was stirred at room temperature with M-MIL-101-NH$_2$ (M = Cr, Al) to generate compounds **1** and **2**, respectively. Compound **3** was synthesised by refluxing peda and Cr-MIL-101-NH$_2$ in toluene for 16 h. Characterisation of PSM products by FTIR, ^{1}H NMR, PXRD and surface area measurements were consistent with 100% conversion in each case. PXRD measurements also confirmed the retention of crystallinity (Figure S3). The broadness of the peaks, particularly for the aluminium analogue is not unusual for large pore frameworks such as MIL-101, and the PXRD patterns presented here compare well to others in the literature for frameworks of this structure type.[19, 21, 29-31] FTIR spectroscopy indicated that PSM had occurred successfully through the emergence of peaks corresponding to the newly introduced functionalities (Figure S4a). The percentage of ligand conversion in compounds **1** and **2** was determined using solution state ^{1}H NMR of the decomposed product in NaOH/D$_2$O (Figure S4b). Additionally, for compounds **1** and **2**, a step in the TGA at *ca.* 150 °C indicated thermolysis of the BOC group of the BOC-Arg-OH moiety (this step was not

COMMUNICATION

present in the TGAs of the parent compounds Cr-MIL-101-NH$_2$ and Al-MIL-101-NH$_2$) (Figure S5).

For compound **1**, the UV-visible spectrum of the post-synthetically modified compound was slightly red shifted compared to that of the parent compound (Cr-MIL-101-NH$_2$),

but otherwise exhibited identical absorption features (Figure S6). The red shift is the result of a decrease in energy of the MLCT band involving the Cr^{3+}. Compound **1** also displays a less intense absorption band at 390 nm than the corresponding band in Cr-MIL-101-NH$_2$; this is likely due to a change in the
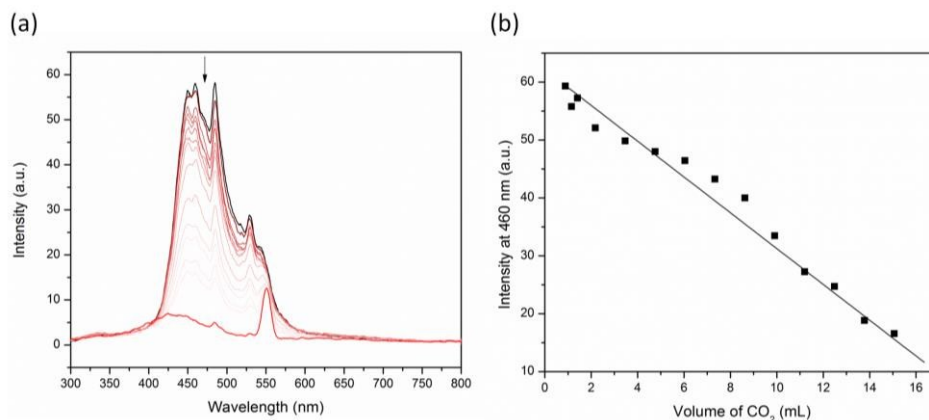

Figure 2 (a) Fluorescence response of a suspension of **1** in water degassed with Ar (black) and with incremental CO$_2$ dosing (red) following excitation at 275 nm, and (b) intensity at 460 nm *vs.* volume of CO$_2$ dosed.

electronic properties of the ligand upon PSM from a strongly electron-donating NH$_2$ group to a moderately electron-donating NHCOR (amide) group. For **2**, the UV-visible spectra of the parent and PSM compounds are identical, reflecting the lack of absorption features in the UV-visible spectrum of arginine itself (Figure S6). The UV-visible spectrum of compound **3** is similar to that of the introduced peda moiety; in particular, the broad feature from 450–550 nm reflects the change in colour of the framework from green to red (Figure S6).

A summary of the gas adsorption properties for compounds **1–3** is provided in **Error! Reference source not found.**. Surface area measurements indicated that accessible surface area remained following PSM in all cases, despite the sizes of the moieties incorporated during PSM (Figure S7, **Error! Reference source not found.**). Additionally, a degree of mesoporosity was retained in all cases, as evidenced by the Type IV adsorption isotherms[32] and the pore size distribution data shown in Figure S8.

In all compounds **1–3**, a decrease in the CO$_2$ uptake was observed when compared to Cr-MIL-101; this may be an indicator of weaker framework-CO$_2$ affinities compared with the parent framework, as systems with small pores in which the potential wells overlap generally *increase* CO$_2$ uptake. Compounds **1** and **2** had comparable CO$_2$ uptakes at <200 mbar; however, compound **2** had a significantly higher uptake at 1 bar (Figure S9). Compound **3** exhibited relatively low uptake at all pressures from 0–1 bar, which is likely the result of significantly reduced surface area and increased disruption to the crystalline lattice in this compound. The trend in CO$_2$ uptake at 1 bar follows that of the surface area and pore volume, indicating that limited interactions were occurring between CO$_2$ and the functional groups in each case. The H$_2$ uptake at 77 K (Figure S9) and CO$_2$ uptake at 195 K (Figure S10)

both follow the same trend as that of the CO$_2$ uptake at 298 K, which is to be expected given the relationship between surface area/pore volume and gas uptake in compounds **1–3**. The heats of adsorption for compounds **1–3** are all higher than that of the parent framework MIL-101-NH$_2$ (26.8–34.7 *vs.* 25.1 kJ/mol, respectively). The magnitude of the CO$_2$ heat of adsorption data indicated that there were no significant interactions between CO$_2$ and the introduced functionalities (Figure S11). This is unusual given that interactions between the nitrogen lone pair of the amine or amidine pore functionality and CO$_2$ may be expected to be on the order of magnitude of a strong physisorption or weak-moderate chemisorption interaction previously reported for such *N*-donors;[23, 25-28, 33] however, this may indicate a difference in reactivity under dry and humid conditions.

Upon investigating the interplay between the fluorescence and CO$_2$ adsorption properties of compounds **1–3**, a quenching of the fluorescence peaks in all cases upon exposure to CO$_2$ was observed. This behaviour was unexpected as amidine-based ionic liquids and amine-perylene polymer conjugates have previously been shown to turn *on* their fluorescence response upon exposure to dissolved CO$_2$ in aqueous media (Figures S12–S14).[7, 8] The solid-state interactions may differ from those in the solution-state as changes in the optical properties of materials in solution may result from intermolecular aggregation (which may arise, for example, due to the change in the protonation state of the fluorophore); such interactions do not occur in the solid state. Small amounts of water present in the solvent may also play a role in the reactivity of these moieties with CO$_2$.

To investigate the possible role of solvent in the reactivity of compounds **1–3** with CO$_2$, UV-visible and fluorescence experiments were conducted on the frameworks suspended in H$_2$O and DMF. The intensity at the maximum emission

wavelength was monitored with increased CO_2 dosing, as many fluorescence-based CO_2 sensors are designed to directly monitor intensity at a specified wavelength.[2] The suspensions of all three materials behaved similarly to the materials under dry conditions, and showed fluorescence quenching upon the introduction of CO_2. Compound **1** suspended in H_2O showed a red-shifted emission at 475 nm (rather than at 435 nm

observed in the solid-state experiment). As shown in Figure 2, the introduction of CO_2 resulted in a decrease in the emission intensity at 460 nm, while a "shoulder" peak at 410 nm increased in intensity. The intensity decreases linearly with increasing CO_2 dosing.
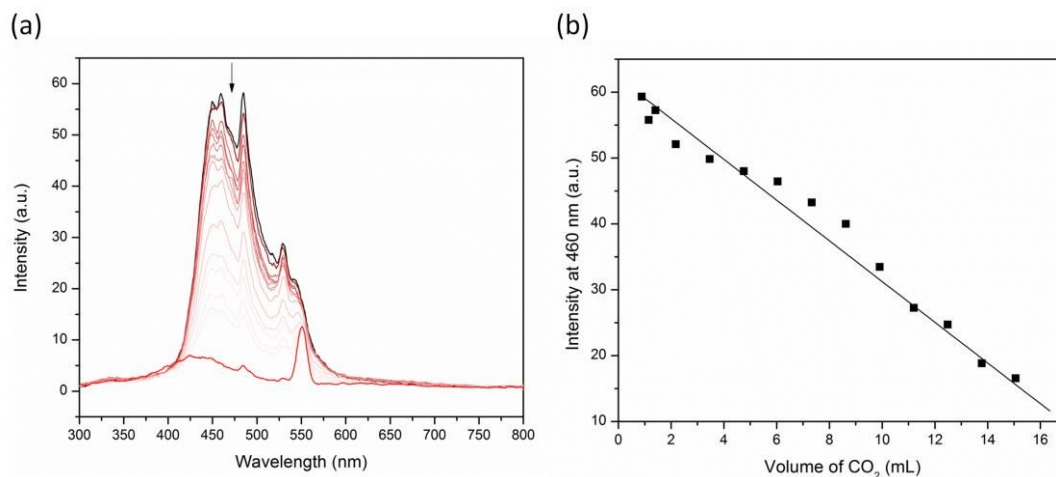

Figure 3 (a) Fluorescence response of a suspension of **1** in DMF degassed with Ar (black) with incremental CO_2 dosing (red) following excitation at 275 nm, and (b) intensity at 460 nm *vs*. volume of CO_2 dosed

As shown in **Error! Reference source not found.**, a decrease in the emission intensity of **1** was also observed in DMF upon CO_2 dosing. The fluorescence quenching in DMF (75%) and water (73%) were comparable and within experimental error of one another. Compound **2** suspended in H_2O also showed linear fluorescence quenching upon the introduction of CO_2 (as it did in the solid-state measurements); however, the extent of fluorescence quenching tapered after 30 min (Figure S15). This may be the result of a limit to the degree of quenching being reached, *i.e.,* the detection limit of the MOF. For compound **2** suspended in DMF (which has a higher CO_2 solubility), no plateau was observed in the fluorescence quenching (Figure S16), and the linear relationship between fluorescence quenching and increased CO_2 dosing was less distinct than for compound **1** (R^2 values given in

Table **2**). A summary of the statistical values from the linear regressions from graphs showing intensity *vs.* volume of CO_2 for compounds **1** and **2** are provided in

Table **2**.

Compound **3** suspended in H_2O similarly exhibited fluorescence quenching upon introduction of CO_2 (Figure S17); however, after 5 min the fluorescence intensity began to *increase* with time. This may be due to the weak nature of the initial fluorescence emission, which results in a large degree of error in measurements of differences in fluorescence over time due to coordination of the perylene fluorophore onto the quenching Cr^{3+} metal site. A similar effect was observed for

compound **3** in DMF (Figure S18), whereby the weak fluorescence emission at 390 nm fluctuated significantly with CO_2 dosing such that no distinct relationship could be derived. Again, the unusual non-linear response to CO_2 dosing may be due to the weak initial fluorescence, resulting in a large degree of error in the measurements.

Table 2 Summary of linear regression slopes and R^2 values from graphs of fluorescence intensity *vs.* volume of CO_2 for compound **1–3** in H_2O and DMF

Sample	Solvent	Slope of linear regression	R^2 value of linear regression
1	H_2O	-2.13	0.97
1	DMF	-0.80	0.97
2	H_2O	-1.04	0.92
2	DMF	-0.26	0.91

Conclusions

Together, the data suggest that the strategy of including strong CO_2-interaction sites (in this case, amines and amidines) is a useful one for the synthesis of CO_2 fluorophoric chemosensors, as both compounds **1** and **2** showed a moderately strong linear relationship between amount of CO_2 and degree of fluorescence quenching (

Table **2**). It is likely that the perylene strategy was not useful in this case due to the fluorescence quenching by the Cr^{3+} site onto which the perylene was grafted, resulting in only a weak initial fluorescence signal. Potentially, the perylene strategy could be useful as both a colorimetric and fluorophoric sensor provided that peda is coordinated to a metal centre that does not quench the fluorescence response. The linear regression data (

Table **2**) indicate that compound **1** is a more effective sensor for dissolved CO_2, as it displays the most pronounced optical response to small quantities of CO_2 (and is therefore a more sensitive detector) and the highest R^2 value (*i.e.*, there is a strong linear correlation between quantity of CO_2 and the degree of optical response). This feature would make it a useful material in reagent-mediated luminescence-based sensors with direct intensity detection. Such methods have been employed in oxygen sensing *via* quenching of the fluorescence of ruthenium polypyridyl or porphyrin complexes, allowing the oxygen partial pressure to be measured as a function of the luminescence intensity of the complex.[2] On the other hand, previously reported fluorescence-based CO_2 sensors have been based on ratiometric sensing,[34] which is a self-referencing technique whereby either an analyte-insensitive emission band of the dye is ratioed with an analyte-dependent band. This technique is superior to simple direct intensity direction, and presents a possible future direction of

the present work (e.g., through the incorporation of both CO_2-reactive and CO_2-unreactive fluorescent moieties into a single MOF).

While absorption-based (colorimetric) CO_2 sensing is another fruitful avenue,[35, 36] luminescence is intrinsically more sensitive, and offers higher sensitivity than absorption-based sensors. Another issue not addressed here is the reliance of many CO_2 sensors on changes in pH, rather than directly "sensing" CO_2 itself (as such, many commercial sensors for dissolved CO_2 rely on Henry's law and are based on CO_2 partial pressures).[37] The materials explored in the present work leeched the grafted arginine (in the case of **1** and **2**) or peda (in the case of **3**) molecules into solution upon exposure to acid (HCl) or base (NaOH); hence, their specificity for CO_2 could not be determined. Given the optical response of both the arginine and peda moieties to acid and base, it is reasonable to assume that a MOF stable to these conditions would not be CO_2-specific, but rather, would act as a general pH sensor. To prevent the ingress of protons and avoid cross-reactivity between pH and CO_2, hydrophobic coatings on multilayer sol-gel structures have been applied,[38] and a similar principle has recently been applied to MOFs to increase hydrophobicity.[39] Evidently, many opportunities exist to expand upon the present work which has demonstrated how the multifunctionality in MOFs may be exploited to develop a sensitive CO_2 chemosensor.
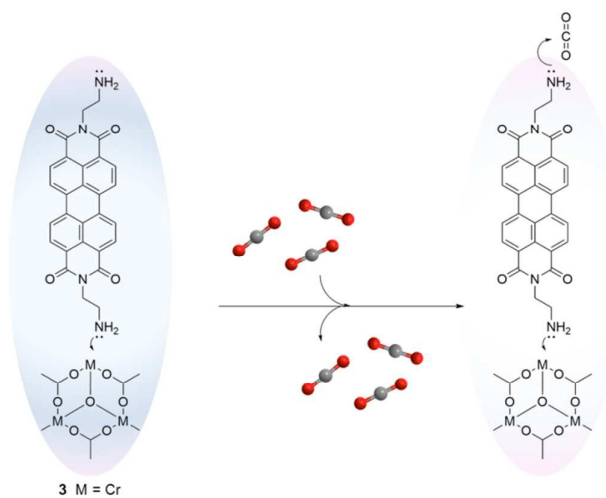
Notes and references

1   A. Mills and S. Hodgen, *Topics in Fluorescence Spectroscopy*, 2005, 119-161.

2   C. McDonagh, C. S. Burke and B. D. MacCraith, *Chemical Reviews*, 2008, **108**, 400-422.

3   D. M. D'Alessandro, B. Smit and J. R. Long, *Angewandte Chemie-International Edition*, 2010, **49**, 6058-6082.

4   K. Sumida, D. L. Rogow, J. A. Mason, T. M. McDonald, E. D. Bloch, Z. R. Herm, T.-H. Bae and J. R. Long, *Chemical Reviews*, 2012, **112**, 724-781.

5   N. Yanai, K. Kitayama, Y. Hijikata, H. Sato, R. Matsuda, Y. Kubota, M. Takata, M. Mizuno, T. Uemura and S. Kitagawa, *Nature Materials*, 2011, **10**, 787-793.

6   Y. Liu, Y. Tang, N. N. Barashkov, I. S. Irgibaeva, J. W. Y. Lam, R. Hu, D. Birimzhanova, Y. Yu and B. Z. Tang, *Journal of the American Chemical Society*, 2010, **132**, 13951-13953.

7   T. Tian, X. Chen, H. Li, Y. Wang, L. Guo and L. Jiang, *Analyst*, 2013, **138**, 991-994.

8   L. Q. Xu, B. Zhang, M. Sun, L. Hong, K.-G. Neoh, E.-T. Kang and G. D. Fu, *Journal of Materials Chemistry A*, 2013, **1**, 1207-1212.

9   J. Y. Quek, T. P. Davis and A. B. Lowe, *Chemical Society Reviews*, 2013, **42**, 7326-7334.

10   H. Jeazet, T. Koschine, C. Staudt, K. Raetzke and C. Janiak, *Membranes*, 2013, **3**, 331.

11   P. G. Jessop, S. M. Mercer and D. J. Heldebrant, *Energy & Environmental Science*, 2012, **5**, 7240-7253.

12   S. Lin and P. Theato, *Macromolecular Rapid Communications*, 2013, **34**, 1118-1133.

13   Z. Guo, Y. Feng, S. He, M. Qu, H. Chen, H. Liu, Y. Wu and Y. Wang, *Advanced Materials*, 2013, **25**, 584-590.

14   Q. Yan, R. Zhou, C. Fu, H. Zhang, Y. Yin and J. Yuan, *Angewandte Chemie*, 2011, **123**, 5025-5029.

15   T. A. Darwish, R. A. Evans, M. James and T. L. Hanley, *Chemistry – A European Journal*, 2011, **17**, 11399-11404.

16   S. Bhattacharjee, C. Chen and W.-S. Ahn, *RSC Advances*, 2014, **4**, 52500-52525.

17   B. Roy, T. Noguchi, D. Yoshihara, Y. Tsuchiya, A. Dawn and S. Shinkai, *Organic & Biomolecular Chemistry*, 2014, **12**, 561-565.

18   G. Férey, C. Mellot-Draznieks, C. Serre, F. Millange, J. Dutour, S. Surblé and I. Margiolaki, *Science*, 2005, **309**, 2040-2042.

19   T. Čendak, E. Žunkovič, T. U. Godec, M. Mazaj, N. Z. Logar and G. Mali, *The Journal of Physical Chemistry C*, 2014, **118**, 6140-6150.

20   E. Valeur and M. Bradley, *Chemical Society Reviews*, 2009, **38**, 606-631.

21   H. Hintz and S. Wuttke, *Chemical Communications*, 2014.

22   R. K. Deshpande, J. L. Minnaar and S. G. Telfer, *Angewandte Chemie*, 2010, **122**, 4702-4706.

23   A. Demessence, D. M. D'Alessandro, M. L. Foo and J. R. Long, *Journal of the American Chemical Society*, 2009, **131**, 8784-8786.

24   Y. K. Hwang, D.-Y. Hong, J.-S. Chang, S. H. Jhung, Y.-K. Seo, J. Kim, A. Vimont, M. Daturi, C. Serre and G. Férey, *Angewandte Chemie, International Edition*, 2008, **47**, 4144-4148.

25 T. M. McDonald, D. M. D'Alessandro, R. Krishna and J. R. Long, *Chemical Science*, 2011, **2**, 2022-2028.

26 T. M. McDonald, W. R. Lee, J. A. Mason, B. M. Wiers, C. S. Hong and J. R. Long, *Journal of the American Chemical Society*, 2012, **134**, 7056-7065.

27 A. Das, M. Choucair, P. D. Southon, J. A. Mason, M. Zhao, C. J. Kepert, A. T. Harris and D. M. D'Alessandro, *Microporous and Mesoporous Materials*, 2013, **174**, 74-80.

28 A. Das, P. D. Southon, M. Zhao, C. J. Kepert, A. T. Harris and D. M. D'Alessandro, *Dalton Transactions*, 2012, **41**, 11739-11744.

29 S. Wuttke, C. Dietl, F. M. Hinterholzinger, H. Hintz, H. Langhals and T. Bein, *Chemical Communications*, 2014, **50**, 3599-3601.

30 G. Akiyama, R. Matsuda, H. Sato, A. Hori, M. Takata and S. Kitagawa, *Microporous and Mesoporous Materials*, 2012, **157**, 89-93.

31 S. Bernt, V. Guillerm, C. Serre and N. Stock, *Chemical Communications*, 2011, **47**, 2838-2840.

32 M. Thommes, K. Kaneko, A. V. Neimark, J. P. Olivier, F. Rodriguez-Reinoso, J. Rouquerol and K. S. Sing, *Pure and Applied Chemistry*, 2015, **87**, 1051-1069.

33 P. Cui, Y.-G. Ma, H.-H. Li, B. Zhao, J.-R. Li, P. Cheng, P. B. Balbuena and H.-C. Zhou, *Journal of the American Chemical Society*, 2012, **134**, 18892-18895.

34 Q. Zhu, R. C. Aller and Y. Fan, *Marine Chemistry*, 2006, **101**, 40-53.

35 H. Segawa, E. Ohnishi, Y. Arai and K. Yoshida, *Sensors and Actuators B: Chemical*, 2003, **94**, 276-281.

36 O. Oter, K. Ertekin, D. Topkaya and S. Alp, *Sensors and Actuators B: Chemical*, 2006, **117**, 295-301.

37 MEP Instruments, 2015.

38 D. A. Nivens, M. V. Schiza and S. M. Angel, *Talanta*, 2002, **58**, 543-550.

39 W. Zhang, Y. Hu, J. Ge, H.-L. Jiang and S.-H. Yu, *Journal of the American Chemical Society*, 2014, **136**, 16978-16981.

Graphical Abstract

3 M = Cr

An amidine-functionalised metal-organic framework (MOF) was shown to be an effective chemosensor in the presence of gaseous and aqueous phase CO_2.